Amino Acids (2013) 44:631–644
DOI 10.1007/s00726-012-1387-7

ORIGINAL ARTICLE

eIF5A dimerizes not only in vitro but also in vivo and its molecular envelope is similar to the EF-P monomer

Camila Arnaldo Olhê Dias · Wanius Garcia · Cleslei Fernando Zanelli · Sandro Roberto Valentini

Received: 6 January 2012 / Accepted: 1 August 2012 / Published online: 4 September 2012

Abstract The protein eukaryotic initiation factor 5A (eIF5A) is highly conserved among archaea and eukaryotes, but not in bacteria. Bacteria have the elongation factor P (EF-P), which is structurally and functionally related to eIF5A. eIF5A is essential for cell viability and the only protein known to contain the amino acid residue hypusine, formed by post-translational modification of a specific lysine residue. Although eIF5A was initially identified as a translation initiation factor, recent studies strongly support a function for eIF5A in the elongation step of translation. However, the mode of action of eIF5A is still unknown. Here, we analyzed the oligomeric state of yeast eIF5A. First, by using size-exclusion chromatography, we showed that this protein exists as a dimer in vitro, independent of the hypusine residue or electrostatic interactions. Protein–protein interaction assays demonstrated that eIF5A can form oligomers in vitro and in vivo, in an RNA-dependent manner, but independent of the hypusine residue or the ribosome. Finally, small-angle X-ray scattering (SAXS) experiments confirmed that eIF5A behaves as a stable dimer in solution. Moreover, the molecular envelope determined from the SAXS data shows that the eIF5A dimer is L-shaped and superimposable on the tRNA^{Phe} tertiary structure, analogously to the EF-P monomer.

Keywords eIF5A · Dimer · Hypusine · EF-P · tRNA

Introduction

The putative eukaryotic translation initiation factor 5A (eIF5A) is a small (17 kDa) acidic protein, highly conserved and essential among archaea and eukaryotes, but not in bacteria (Schnier et al. 1991; Chen and Liu 1997; Park et al. 1997). Alternatively, bacteria have an eIF5A ortholog, elongation factor P (EF-P), which shares important structural features with eIF5A (Park et al. 2010).

eIF5A is activated by a unique post-translational modification, in which a specific lysine (K51 in yeast) is converted into the unusual amino acid residue hypusine by the enzymes deoxyhypusine synthase and deoxyhypusine hydroxylase (Park et al. 2010). The hypusine modification is essential for the eIF5A function and hypusine and/or deoxyhypusine have been identified in all analyzed archaea and eukaryotes, but not in bacteria (Park et al. 2010).

EF-P does not contain the hypusine residue. However, in a subset of bacterial species, the enzymes lysyl-tRNA synthetase (YjeA) and lysine-2,3-aminomutase (YjeK) modify EF-P post-translationally with the addition of a β-lysine at its lysine 34, the residue corresponding to the hypusine modification site of eIF5A (Navarre et al. 2010; Yanagisawa et al. 2010; Bailly and de Crécy-Lagard 2010; Roy et al. 2011; Park et al. 2012). This EF-P modification, called β-lysylation, is analogous to the hypusine modification of eIF5A and essential for the EF-P function and cell growth of *E. coli* (Yanagisawa et al. 2010; Park et al. 2012).

Electronic supplementary material The online version of this article (doi:10.1007/s00726-012-1387-7) contains supplementary material, which is available to authorized users.

C. A. O. Dias · C. F. Zanelli · S. R. Valentini (✉)
Department of Biological Sciences, School of Pharmaceutical Sciences, UNESP-Univ Estadual Paulista, Rodovia Araraquara-Jaú, km 01, Araraquara, SP 14801-902, Brazil
e-mail: valentsr@fcfar.unesp.br

W. Garcia
Center of Natural Sciences and Humanities, UFABC-Univ Federal do ABC, Santo André, SP, Brazil

The eIF5A protein was initially characterized as a translation initiation factor, based on its activity in stimulating the formation of methionyl-puromycin in vitro (Kemper et al. 1976; Benne and Hershey 1978; Hershey et al. 1990). Since eIF5A depletion in yeast caused a partial decrease in cell protein synthesis (30 %) and an increase in the number of G1-arrested cells (Kang and Hershey 1994), it was hypothesized that eIF5A was important for the translation of mRNAs encoding specific proteins such as those required for cell cycle progression (Kang and Hershey 1994; Park et al. 1993). In support of this idea, eIF5A function is essential for polarized growth, a process necessary for the G1/S transition in budding yeast (Zanelli and Valentini 2005). Furthermore, synthetic lethality was revealed between mutants of eIF5A and of Ypt1, which is a protein essential for vesicular trafficking and also for proper polarized growth in yeast (Frigieri et al. 2007, 2008). However, the mechanism triggered by eIF5A to accomplish this cell cycle function is still unknown.

More recently, it has been demonstrated that eIF5A interacts physically with the 80S ribosome as well as with the translation elongation factors eEF1A and eEF2 (Jao and Chen 2006; Zanelli et al. 2006). eIF5A was shown to co-fractionate with monosomes in a translation-dependent manner. Moreover, eIF5A mutant strains show accumulation of polysomes instead of polysome run-off and an increase in the average time necessary for ribosomes to transit along mRNAs (Gregio et al. 2009; Saini et al. 2009). In addition, it was demonstrated that eIF5A interacts functionally with the elongation factor eEF2 (Dias et al. 2012). These results strongly support a function for eIF5A in the elongation step of translation rather than the initiation, although it is still not known whether eIF5A affects the translation of all mRNAs or a subset of specific mRNAs.

The three-dimensional structures of eIF5A proteins from archaea (PDB IDs 1eif, 2eif, 1iz6, 1bkb), *Leishmania* species (PDB IDs 1x6o, 1xtd), yeast (PDB ID 3er0) and human (PDB ID 3cpf) exhibit only minor differences (Tong et al. 2009). The analysis of these structures shows that eIF5A is composed of two predominantly β-sheet domains. The N-terminal domain bears the hypusine residue in an exposed loop. This domain is folded in an SH3-like barrel found in other proteins related to translation and harbors a KOW motif proposed to mediate RNA binding (http://supfam.org/SUPERFAMILY; Gough et al. 2001). The C-terminal domain forms an OB-fold, which is also present in other translational machinery components (e.g., eIF1A, eIF2α and several ribosomal proteins) and belongs to the nucleic acid-binding protein superfamily (http://scop.mrc-lmb.cam.ac.uk/scop; Tong et al. 2009).

Interestingly, not only are the primary sequences of eIF5A and EF-P related, but the tertiary structures of EF-P domains I and II are superimposable on the structures of the N-terminal and C-terminal domains of eIF5A, respectively (Hanawa-Suetsugu et al. 2004; Tong et al. 2009). Similarly to eIF5A, EF-P stimulates the formation of a peptide bond between the initiator tRNA and puromycin in vitro, but has no effect on the rate of poly (U)-dependent poly(Phe) synthesis (Benne and Hershey 1978; Glick et al. 1979). EF-P is L-shaped and resembles a tRNA in structure and size (Hanawa-Suetsugu et al. 2004). Recently, the structure of EF-P bound to the 70S ribosome was reported revealing that EF-P binds to a site located between the binding sites for the peptidyl tRNA (P site) and the exiting tRNA (E site) (Blaha et al. 2009). It was proposed that EF-P facilitates the proper positioning of the fMet-tRNA$_i^{fMet}$ for the formation of the first peptide bond during translation initiation (Blaha et al. 2009). As we do not know where eIF5A binds to the ribosome, it remains to be elucidated whether eIF5A functionally mimics EF-P on ribosomes.

Early studies suggested that human eIF5A purified from erythrocytes exists as a dimer in solution and is able to form higher oligomers (Chung et al. 1991). Recently, another group supported the idea that yeast eIF5A is a dimer in vitro and that the dimerization depends on the presence of the hypusine residue and RNA (Gentz et al. 2009). To confirm the ability of the hypusine residue to promote eIF5A oligomerization in vitro, we produced recombinant yeast eIF5A proteins, containing the hypusine residue or not, and performed size-exclusion molecular chromatography under various conditions. We found that eIF5A is a dimer in vitro, independently of the hypusine residue or electrostatic interactions. Moreover, we demonstrated that eIF5A is able to form oligomers in cell extracts and may exist as a dimer in vivo, in a manner that depends on RNA, but not on assembled 80S ribosome or the hypusine residue. Interestingly, the molecular envelope of the eIF5A dimer, analyzed by small-angle X-ray scattering (SAXS), is L-shaped and resembles the tRNA^{Phe} in structure and size, analogously to the EF-P monomer.

Materials and methods

All yeast strains and plasmids used in this study are listed in Online Resource Tables 1 and 2, respectively. All chemicals used in this study were of analytical grade.

Purification of the recombinant yeast protein eIF5A from bacteria

The DNA fragments containing the gene encoding eIF5A (*TIF51A*), Dys1 (*DYS1*) and Lia1 (*LIA1*) were PCR-amplified from the *S. cerevisiae* genome and cloned into

the expression plasmid pST39 as described by Park et al. (2011). For protein purification of eIF5A^{Hyp}, *E. coli* BL21(DE3)pLysS cells transformed with pST39-*TIF51A/DYS1/LIA1* (pVZ1088) were harvested after 4 h of induction with 1 mM isopropyl-β-D-thiogalactopyranoside (IPTG) at 37 °C. The cell pellets from 6 L of culture (20 g) were resuspended in 100 mL of ice-cold lysis buffer (50 mM Tris acetate, 0.1 mM EDTA, 1 mM DTT, containing protease inhibitor cocktail—Roche, adjusted to pH 7.0) and lysed by sonication. The cell lysate was centrifuged at 25,000×*g* for 30 min and the clarified lysate was subjected to a sequence of ion exchange chromatography to obtain eIF5A^{Hyp}, as previously described by Park et al. (2011).

To produce 6xHis-eIF5A^{Lys}, the gene *TIF51A* was amplified from the *S. cerevisiae* genome and cloned into the expression plasmid pQE-30 (Qiagen). The *E. coli* strain M15 was transformed with pQE-*TIF51A* (pSV727) and the recombinant yeast protein 6xHis-eIF5A^{Lys} was overexpressed upon exposure to 0.4 mM IPTG for 4 h at 37 °C. The cell pellet from 2 L of culture was washed twice in cold PBS (140 mM NaCl, 2.7 mM KCl, 10 mM Na_2HPO_4, 1.8 mM KH_2PO_4, adjusted to pH 7.4) and suspended in 20 mL of ice-cold lysis buffer (20 mM NaH_2PO_4, 300 mM NaCl, 20 mM imidazole, 2 mM DTT, 2 mM PMSF, 5 μg/mL of pepstatin, leupeptin, aprotinin and chymostatin, adjusted to pH 8.0). The 6xHis-eIF5A^{Lys} fusion protein was purified by affinity chromatography on Ni–NTA resin, as recommended by the manufacturer (Qiagen). Clones encoding 6xHis-eIF5A^{G50A}, 6xHis-eIF5A^{K51R}, 6xHis-eIF5A^{K56A} and 6xHis-eIF5A^{K56D} were constructed using a site-directed mutagenesis kit, as recommended by the manufacturer (Stratagene), and the recombinant proteins without the hypusine residue were purified by the same method used to purify 6xHis-eIF5A^{Lys}.

Purification of the recombinant yeast proteins 6xHis-eIF5A and 6xHis-eIF5A^{K51R} from yeast

The same DNA fragment encoding yeast eIF5A was cloned into the expression plasmid pYES2 (Invitrogen). The plasmid pYES-6xHis-eIF5A (pVZ975) was then subjected to site-directed mutagenesis to obtain a plasmid encoding 6xHis-eIF5A^{K51R} (pVZ976). The clones were introduced into the SVL55 yeast strain to overproduce yeast 6xHis-eIF5A^{Hyp} (containing the hypusine residue) or 6xHis-eIF5A^{K51R} (not containing the hypusine residue) in yeast. The resulting strains were grown at 30 °C until they reached an optical density of 0.4 at 600 nm, when the production of recombinant fusion protein was induced by adding 2 % galactose and waiting for 15 h. Cells were collected, washed twice in 20 mL of cold PBS and suspended in 40 mL of cold buffer (20 mM NaH_2PO_4, 300 mM NaCl, 20 mM imidazole, 2 mM DTT, 2 mM PMSF, 5 μg/mL of pepstatin, leupeptin, aprotinin and chymostatin, adjusted to pH 8.0). After lysis in a French press, the cell lysate was centrifuged and the fusion protein purified by affinity chromatography on Ni–NTA resin, as recommended by the manufacturer (Qiagen).

Size-exclusion molecular chromatography of eIF5A

The recombinant yeast proteins, eIF5A^{Hyp} and 6xHis-eIF5A^{Lys} (wild-type or mutants), were purified from *E. coli* by ion exchange or affinity chromatography, as described above. SDS-PAGE gels of 6xHis-eIF5A^{Lys} and eIF5A^{Hyp} are presented in Online Resource Figs. 1 and 2. After concentration of the protein to 2 mg/mL in a buffer containing 20 mM Tris–HCl (pH 7.5), 0.1 mL of the protein solution was separated on a 70 mL Superdex 75 column (GE Life Science). The molecular mass standard proteins (GE Life Science) ribonuclease A (13.7 kDa) and ovalbumin (43.0 kDa), each at a concentration of 2 mg/mL, were used to calibrate the column. The elution buffer used was 20 mM Tris–HCl (pH 7.5) with or without 500 mM NaCl and 10 mM DTT. The proteins 6xHis-eIF5A^{Hyp} and 6xHis-eIF5A^{K51R} were purified from yeast (Online Resource Fig. 2), as described above, and subjected to size-exclusion molecular chromatography. The proteins, at 0.5 mg/mL, in a buffer containing 20 mM Tris–HCl (pH 7.5) and 100 mM NaCl, were separated on a 90 mL Superdex 200 column (G.E. Life Science). Ribonuclease A (13.7 kDa), chymotrypsinogen A (25 kDa), ovalbumin (43 kDa) and albumin (67 kDa) were used as mass standard proteins, each at a concentration of 2 mg/mL (G.E. Life Science). The void volume of each column was calculated with Blue Dextran 2000. Eluted eIF5A proteins were collected and analyzed by SDS-PAGE and Western blot with a polyclonal anti-eIF5A antibody.

GST pull-down assay followed by mass spectrometry analysis

Plasmids expressing GST alone (pSV20) or GST-eIF5A (pSV36) were introduced into the wild-type strain SVL55. The resulting strains were used for GST pull-down assays. Briefly, cells were grown at 30 °C to $OD_{600nm} = 0.4$ and production of GST fusion proteins was induced with 2 % galactose for 3 h. Cells were collected, washed twice in cold PBS and suspended in cold Buffer A (30 mM HEPES, 100 mM KAc, 2 mM MgAc, 7 mM β-mercaptoethanol, 5 μg/mL of pepstatin, leupeptin, aprotinin and chymostatin, adjusted to pH 7.5). Cells were broken by vortexing with glass beads for 3 min, and incubating the tubes in an ice bath for 1 min after each 1 min vortex. Cell lysates were clarified by centrifugation at 20,000×*g* for 20 min at

4 °C, and total protein concentration was determined by the Bradford method. Clarified lysates (2 mg) were incubated with 100 µL of glutathione Sepharose beads (50 % slurry) for 1 h, at 4 °C. Beads were collected, washed five times with cold Buffer A, and the bound proteins eluted in 50 µL of Buffer B (50 mM Tris–HCl, 100 mM NaCl, 3 % L-glutathione reduced, adjusted to final pH 8.0). After separation by SDS-PAGE, proteins were visualized by silver staining. In order to identify the copurified proteins, the bands of interest were excised and subjected to in-gel tryptic digestion, as described by William et al. (1997). The resulting peptide mixtures were extracted and analyzed by MALD-ToF mass spectrometry.

GST pull-down assay followed by Western blot analysis

A yeast strain producing ProtA-eIF5A as the sole source of eIF5A (SVL731) was transformed with the following pairs of plasmids: pSV36 (GST-eIF5A) + pSV146 (eIF5A); pSV40 (GST-eIF5A^{K51R}) + pSV39 (eIF5A^{K51R}) and pSV20 (GST) + pSV146 (eIF5A). The resulting strains were used for GST pull-down assays. Briefly, cells were grown at 30 °C until $OD_{600nm} = 0.4$ and then the production of GST fusion proteins was induced by 2 % galactose for 3 h. Cells were collected, washed twice in cold PBS and suspended in cold Buffer A (described above). Cells were lysed by vortexing with glass beads for 3 min and incubating the tubes in an ice bath for 1 min after every 1 min of vortex. Cell lysates were clarified by centrifugation at 20,000×*g* for 20 min at 4 °C, and the total protein concentration was determined by Bradford assay. Clarified lysates (2 mg of total protein) were incubated with 100 µL of glutathione-Sepharose beads (50 % slurry) for 1 h, at 4 °C. Unbound fractions were collected, and the beads were washed five times with cold Buffer A and suspended in 30 µL of SDS-PAGE loading buffer. Bound and unbound fractions were separated by SDS-PAGE (12 % gel) and analyzed by Western blot, using polyclonal anti-eIF5A antibody. Where indicated, RNase was added at 300 mg/mL and EDTA at 40 mM.

GST pull-down assay using purified proteins

The same DNA fragment encoding yeast eIF5A was cloned into the expression plasmid pGEX-4T (G.E. Life Science). The *E. coli* strain BL21 was transformed with the plasmids encoding the proteins GST (pGEX-4T) or GST-eIF5A (pSV35) and protein production was induced for 3 h at 37 °C with 0.4 mM IPTG. The harvested cell pellet from 2 L of culture was washed twice in cold PBS and suspended in 20 mL of ice-cold lysis buffer (20 mM Tris–HCl, 5 µg/mL of pepstatin, leupeptin, aprotinin and chymostatin). GST, GST-eIF5A and eIF5A proteins were purified by affinity chromatography on glutathione-Sepharose, as recommended by the resin manufacturer (G.E. Life Science). The fractions containing the protein were collected and concentrated with an Amicon filter (Millipore). A total of 5 µg of GST or GST-fused protein was bound to glutathione-Sepharose beads in PBS for 30 min at 25 °C. After three washes with 1 mL PBS, 1 µg eIF5A protein was added in a volume of 1 mL Buffer X (20 mM Tris–HCl (pH 8.0), 0.5 % Triton X-100) and the reaction mixtures were incubated for 1 h at 4 °C. Unbound fractions were collected and the beads washed three times with 1 mL of Buffer X containing 300 mM NaCl. Bound and unbound fractions were incubated with SDS-PAGE loading buffer for 5 min at 95 °C and separated on a 12 % SDS-polyacrylamide gel by electrophoresis, followed by Western blot with polyclonal anti-eIF5A and anti-GST (Sigma) antibodies.

Small-angle X-ray scattering (SAXS) experiments

The recombinant yeast protein 6xHis-eIF5A^{Hyp} (containing the hypusine residue), purified from yeast as described above, was subjected to SAXS experiments at the concentrations of 2 and 6 mg/mL, in 25 mM Tris–HCl (pH 7.8) containing 20 mM NaCl. The measurements were carried out at the LNLS (National Synchrotron Light Laboratory, Campinas, Brazil) synchrotron SAXS beamline (Kellermann et al. 1997). The 6xHis-eIF5A^{Hyp} samples (250 µL) were centrifuged for 15 min at 14,000×*g* (at 4 °C) prior to the measurements, to remove aggregates or particles, and then placed on ice. The samples were then loaded into cells made of two thin parallel mica windows and kept at room temperature during the measurements. Two successive frames of 300 s each were recorded for each sample to monitor radiation damage and beam stability. The wavelength of the incoming monochromatic X-ray beam was set to $\lambda = 0.148$ nm. The X-ray patterns were recorded with a two-dimensional CCD detector (MarResearch, USA). The sample–detector distance (1031.5 mm) was adjusted to record the scattering intensity over a range of q (scattering vector) values from 0.1 to 3.5 nm^{-1}, where $q = 4\pi \sin(\theta)/\lambda$ and θ is half the scattering angle. Buffer scattering was recorded before each sample scattering. The parasitic scattering from air and beamline windows was subtracted from the total measured intensities. The integration of SAXS patterns was performed with the Fit2D software (Hammerley 1997) and the curves were scaled by protein concentration.

SAXS data analysis

The radius of gyration (Rg) of the molecule was determined by two independent procedures: by the Guinier

equation (Guinier 1955) ($I(q) = I(0).\exp[(-q^2 \times Rg^2)/3]$, $q < 1.3/Rg$) and by the indirect Fourier transform method, using the Gnom package (Svergun et al. 1988; Svergun 1999). The distance distribution function $P(r)$ was also evaluated with Gnom software and the maximum diameter (D_{max}) was obtained. Molecular weights (MW) were estimated by two methods: (2) by determining the absolute scattering intensity using water scattering (primary standard) (Orthaber et al. 2000) and (2) using a novel procedure implemented as a web tool SAXS MoW (www.ifsc.usp.br/~saxs/saxsmow.html; Fischer et al. 2010). The latter procedure does not require the measurement of SAXS intensity on an absolute scale and does not involve a comparison with another SAXS curve determined from a known standard protein. To calculate the forward scattering I(0) on the absolute scale, the known scattering of water, 1.632×10^{-2} cm^{-1} at 288 K, was used (Orthaber et al. 2000).

SAXS ab initio modeling

Dummy atom models (DAMs) were calculated from the experimental SAXS by ab initio procedures implemented in both the Dammin (Svergun 1999; Petoukhov and Svergun 2003) and Gasbor packages (Svergun and Petoukhov 2001). Several runs of ab initio shape determination with different starting conditions led to consistent results as judged by structural similarity of the output model, yielding nearly identical scattering patterns and fitting statistics in a stable and self-consistent process. The resolution was determined from the equation $q = 2\pi/q_{max}$. The Crysol package was used to generate simulated scattering curves from the DAMs (Svergun 1992). Rg and D_{max} were determined with the same package.

Simulated scattering curves and rigid-body modeling

The three-dimensional crystallographic structures of eIF5A from *Saccharomyces cerevisiae* (PDB ID 3er0), *human* (PDB ID 3cpf), *Pyrococcus horikoshii* (PDB ID 1iz6), *Leishmania braziliensis* (PDB ID 1x6o), *L. mexicana* (PDB ID 1xtd), *Methanococcus jannaschii* (PDB IDs 1eif, 2eif) and *Pyrobaculum aerophilum* (PDB ID 1bkb) were used by Crysol package (Svergun 1992) to generate the simulated scattering curves and to determine Rg and D_{max}. The simulated scattering curves were them compared with the experimental SAXS data. Computed scattering curves based on the crystallographic structures of EF-P from *Thermus thermophilus* (PDB ID 1ueb) and $tRNA^{Phe}$ from *Saccharomyces cerevisiae* (PDB ID 4tna) were also generated by Crysol. Rigid-body modeling of the dimer eIF5A from *S. cerevisiae* was performed with the Sasref package (Konarev 2006). The two monomers from the crystallographic structure of this dimer (PDB ID 3er0) were separated and their relative position and orientation were optimized. Crysol was used to generate the simulated scattering curves from the rigid-body model. The 3-D crystallographic structures and ab initio DAMS were superimposed with the Supcomb package (Kozin and Svergun 2001). Superposition figures were generated by the PyMOL program (Delano 2002).

Results and discussion

eIF5A exists as a dimer, not only in vitro but also in vivo, independently of the presence of the hypusine residue or the ribosome, but dependently on RNA

Initially, to analyze the oligomeric state of eIF5A in vitro, we carried out size-exclusion molecular chromatography on the recombinant eIF5A protein in minimal buffer containing 20 mM Tris–HCl (pH 7.5), using a Superdex 75 column of 70 mL. Figure 1a shows the chromatogram obtained with the molecular mass standard protein analysis. The proteins ovalbumin (43.0 kDa) and ribonuclease A (13.7 kDa) eluted in 26.9 mL and 52.9 mL, respectively. Figure 1b shows that 6xHis-$eIF5A^{Lys}$ (not containing the hypusine residue) or $eIF5A^{Hyp}$ (containing the hypusine residue), both purified from bacteria and at a final concentration of 2 mg/mL, eluted in fractions corresponding to a 40 kDa protein, approximately the size expected for the eIF5A dimer, which suggests that eIF5A is a dimer in vitro, independently of the hypusine residue. The same result was observed in the size-exclusion molecular chromatography of 6xHis-$eIF5A^{Lys}$ at 5 mg/mL or 10 mg/mL, using a Superdex 75 column of 25 mL (data not shown), suggesting that the dissociation constant of eIF5A is low and eIF5A is a dimer in the range of protein concentration used in these experiments. Although these results show clearly that dimerization of eIF5A does not depend on the hypusine residue, they are not in agreement with the results published by Gentz et al. (2009), which suggested that the hypusine residue is necessary for eIF5A dimerization in vitro. However, this discrepancy may be due to different experimental conditions.

To investigate the nature of the interactions involved in eIF5A dimerization, we tested whether ionic interactions or cysteine residues are necessary. The same protein sample used in the experiment shown in Fig. 1b (6xHis-$eIF5A^{Lys}$) was subjected to size-exclusion chromatography in minimal buffer containing 500 mM of NaCl, which prevents ionic interactions, and 10 mM of dithiothreitol (DTT), which is a reducing agent that breaks down the disulfide bridges between cysteine residues. No difference was observed between the elution profile of the 6xHis-$eIF5A^{Lys}$

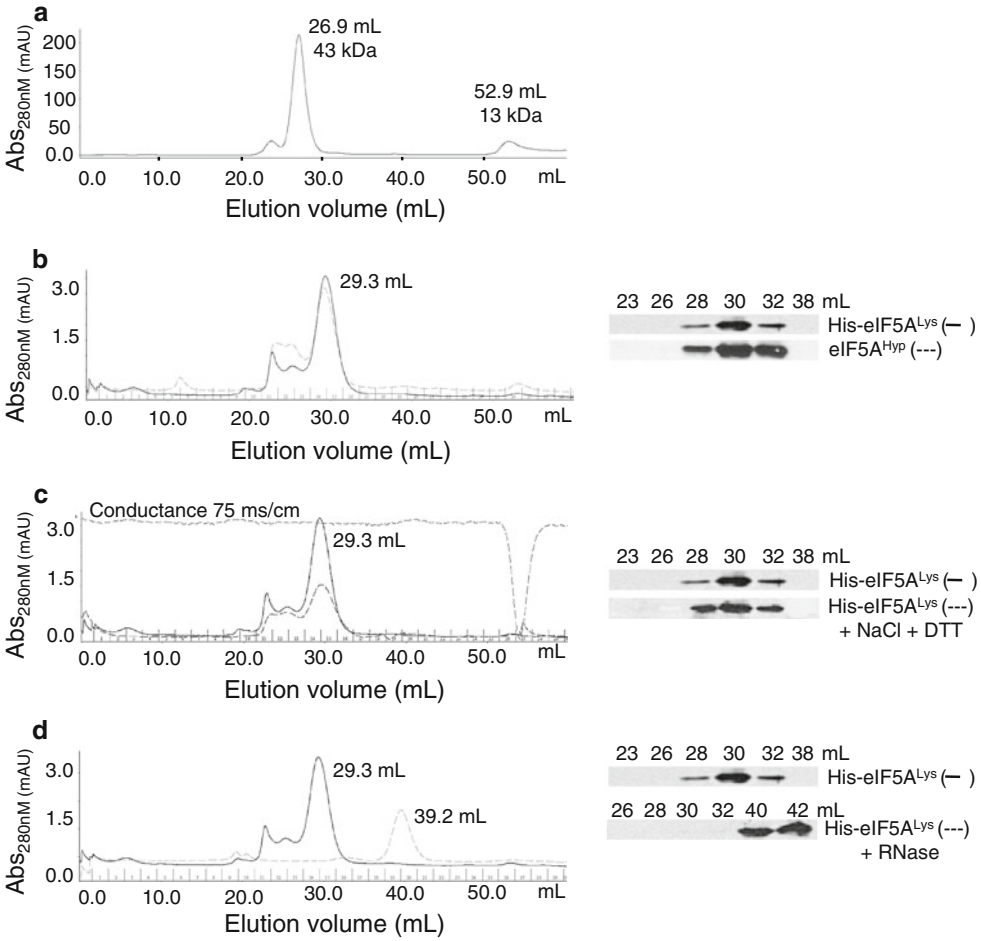

Fig. 1 Effect of the hypusine residue, electrostatic interactions and RNA on dimerization of eIF5A. **a** Size-exclusion chromatography of molecular mass standard proteins ovalbumin (43 kDa) and ribonuclease A (13.7 kDa), using a Superdex 75 column of 70 mL and minimal buffer containing 20 mM Tris–HCl at pH 7.5. **b** Size-exclusion chromatography of 6xHis-eIF5A^{Lys} and 6xHis-eIF5A^{Hyp} in minimal buffer. **c** Size-exclusion chromatography of 6xHis-eIF5A^{Lys} in minimal buffer or with 500 mM NaCl and 10 mM DTT. **d** Size-exclusion chromatograph of 6xHis-eIF5A^{Lys} in minimal buffer, after protein treatment with RNase. All the chromatographic fractions were analyzed by Western blot with eIF5A antibody and are shown beside each chromatogram

under these conditions (Fig. 1c, lower Western blot panel) and that in the first conditions (Fig. 1c, upper Western blot panel), indicating that the oligomeric state of eIF5A does not depend on electrostatic interactions and disulfide bridges in vitro, in agreement with previous studies (Chung et al. 1991; Gentz et al. 2009).

Since the spectroscopic reading at 260 nm of the purified protein showed that 6xHis-eIF5A^{Lys} and eIF5A^{Hyp} were contaminated with RNA from bacteria (Online Resource Fig. 3a, b), we carried out size-exclusion molecular chromatography on 6xHis-eIF5A^{Lys} (2 mg/mL), after its treatment with RNase A (300 mg/mL final concentration), at room temperature for 30 min. As shown in Fig. 1d, lower Western blot panel, 6xHis-eIF5A^{Lys} treated with RNase is eluted in a volume corresponding to a 20 kDa protein, approximately the size expected for the eIF5A monomer, indicating that the eIF5A oligomer in vitro is dependent on RNA. These findings are consistent with previous published data showing the disruption of the eIF5A dimer in vitro in the presence of RNase (Gentz et al. 2009). However, our data suggest that the RNA necessary for dimerization of eIF5A is not specific.

As structural differences may exist between recombinant proteins purified from bacteria and yeast (Prinz et al. 2004), we also analyzed by size-exclusion chromatography the recombinant protein 6xHis-eIF5A^{Hyp} (containing the hypusine residue) and its mutant 6xHis-eIF5A^{K51R} (not containing the hypusine residue), purified from *S. cerevisiae* (Fig. 2). Figure 2a shows the chromatogram obtained with the molecular mass standard protein analysis employing a Superdex 200 column of 90 mL. The proteins, ovalbumin (43.0 kDa) and ribonuclease A (13.7 kDa), are eluted at 81 and 95.7 mL, respectively. Western blot analysis of the chromatographic protein fractions showed that both 6xHis-eIF5A^{Hyp} and 6xHis-eIF5A^{K51R} were eluted in a column volume corresponding to a 40 kDa protein (Fig. 2b), the size expected for the eIF5A dimer. These findings are consistent with the result observed in Fig. 1b and confirm that eIF5A dimerization in vitro is independent of the hypusine residue.

The hypusine loop is strictly conserved throughout eukaryotic evolution and contains either positively charged residues or only uncharged residues. Amino acid substitutions in the hypusine loop cause a total or a severe impairment of deoxyhypusine/hypusine modification and

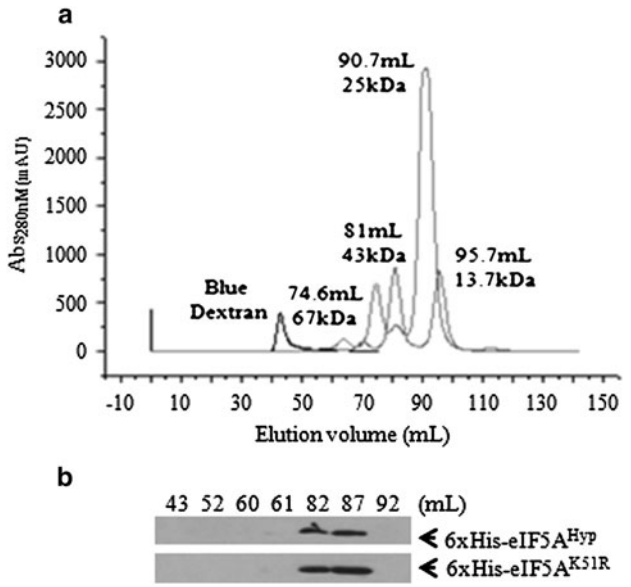

Fig. 2 Effect of hypusine residue on dimerization of 6xHis-eIF5A^{Hyp} and 6xHis-eIF5A^{K51R} purified from yeast. **a** Size-exclusion chromatograph of molecular mass standard proteins albumin (67 kDa), ovalbumin (43 kDa), chymotrypsinogen A (25 kDa) and ribonuclease A (13.7 kDa), using a Superdex 200 column of 90 mL and minimal buffer containing 20 mM Tris–HCl at pH 7.5 and 100 mM NaCl. **b** Analysis of size-exclusion chromatograph fractions by Western blot with eIF5A antibody. *Upper panel* shows the chromatograph fractions of 6xHis-eIF5A^{Hyp} analyses (containing hypusine residue) and *lower panel* shows the chromatograph fractions of 6xHis-eIF5A^{K51R} analyses (not containing hypusine residue). Both analyses were done with the same column and conditions used to analyze the standard proteins

thereby in eIF5A function, especially when the substitution involves insertion of a negatively charged residue (Dias et al. 2008). In order to investigate whether other amino acids in the hypusine loop are necessary to form the eIF5A dimer, size-exclusion molecular chromatography was done with recombinant yeast proteins in which individual amino acids close to the hypusine site have been exchanged (6xHis-eIF5A^{G50A}, 6xHis-eIF5A^{K51R}, 6xHis-eIF5A^{K56A}, 6xHis-eIF5A^{K56D}). For this, we used a Superdex 75 column of 25 mL and the elution volume of these proteins was consistent with the dimeric species observed with the wild-type protein (data not shown), suggesting that the individual amino acid residues around the hypusine site analyzed do not interfere with the oligomeric state of eIF5A either.

To determine whether eIF5A dimerizes not only in vitro but also in vivo, we performed glutathione S-transferase pull-down assay followed by mass spectrometry. GST-eIF5A fusion protein, whose functionality was confirmed by suppressing the temperature sensitivity of an eIF5A mutant (Zanelli et al. 2006), was transiently overexpressed from an inducible high-copy episomal vector. As a negative control, we used another strain expressing GST alone. As shown in Fig. 3a, there is a series of bands corresponding to proteins of different molecular weights that copurify with GST-eIF5A, but not with GST. Several of the most prominent bands, as revealed by silver staining, were identified by mass spectrometry. Ribosomal proteins and the elongation factor 2 (eEF2), already previously identified by our group (Zanelli et al. 2006), were identified again in this study. Interestingly, eIF5A was identified in the region corresponding to 17 kDa (Fig. 3a), which suggests that eIF5A can bind to GST-eIF5A in vivo. In the same protein region, 40S ribosomal proteins S17-A (16 kDa), S19-A (16 kDa), S15 (16 kDa), S18 (17 kDa) and S26 (14 kDa), and 60S ribosomal protein S20 (17 kDa), but not GST were identified. GST was revealed only in the excised protein band corresponding to 26 kDa.

To confirm that eIF5A is able to form oligomers in vivo and, moreover, to check whether the hypusine is important for this interaction, we performed the glutathione S-transferase pull-down experiments with yeast lysates from cells producing GST-eIF5A^{Hyp} + eIF5A^{Hyp} (both containing the hypusine residue), GST-eIF5A^{K51R} + eIF5A^{K51R} (both not containing the hypusine residue) or GST + eIF5A^{Hyp} (negative control) (Fig. 3b). Since eIF5A has been reported to interact with polysomes (Jao and Chen 2006; Zanelli et al. 2006), we also performed GST pull-down experiments in the presence of RNase or EDTA, to disassemble the polysomes. Besides that, the RNase treatment digests free RNA, allowing us to test whether RNA is necessary for eIF5A oligomer formation.

As shown in lane 2 of Fig. 3b, GST alone was unable to interact with eIF5A^{Hyp}. On the other hand, the protein eIF5A^{Hyp} was copurified by GST-eIF5A^{Hyp} (Fig. 3b, lane 4), which supports the idea that eIF5A is able to form oligomers in vivo. In addition, the eIF5A^{K51R} was copurified by GST-eIF5A^{K51R} (Fig. 3b, lane 6), confirming that hypusine modification is not necessary for the oligomerization of eIF5A. Although this assay does not determine which oligomeric state eIF5A assumes (dimer or higher oligomers), the result suggests that eIF5A is an oligomer in vivo, independently of the presence of the hypusine residue. Therefore, the results presented in Fig. 3b are in agreement with those in Figs. 1 and 2, and further support the idea that hypusine modification is not necessary for eIF5A dimerization.

Interestingly, GST-eIF5A^{Hyp} did not pull-down eIF5A-^{Hyp} in the presence of RNase (Fig. 3b, lane 8), suggesting that the formation of the eIF5A oligomer in vivo does depend on RNA, as observed in the eIF5A dimer in vitro (Fig. 1d). In fact, besides the observation that the structure of eIF5A contains oligonucleotide/oligosaccharide-binding fold domains that can bind to DNA and/or RNA (http://supfam.org/SUPERFAMILY; Tong et al. 2009), eIF5A has been reported to bind specific RNA

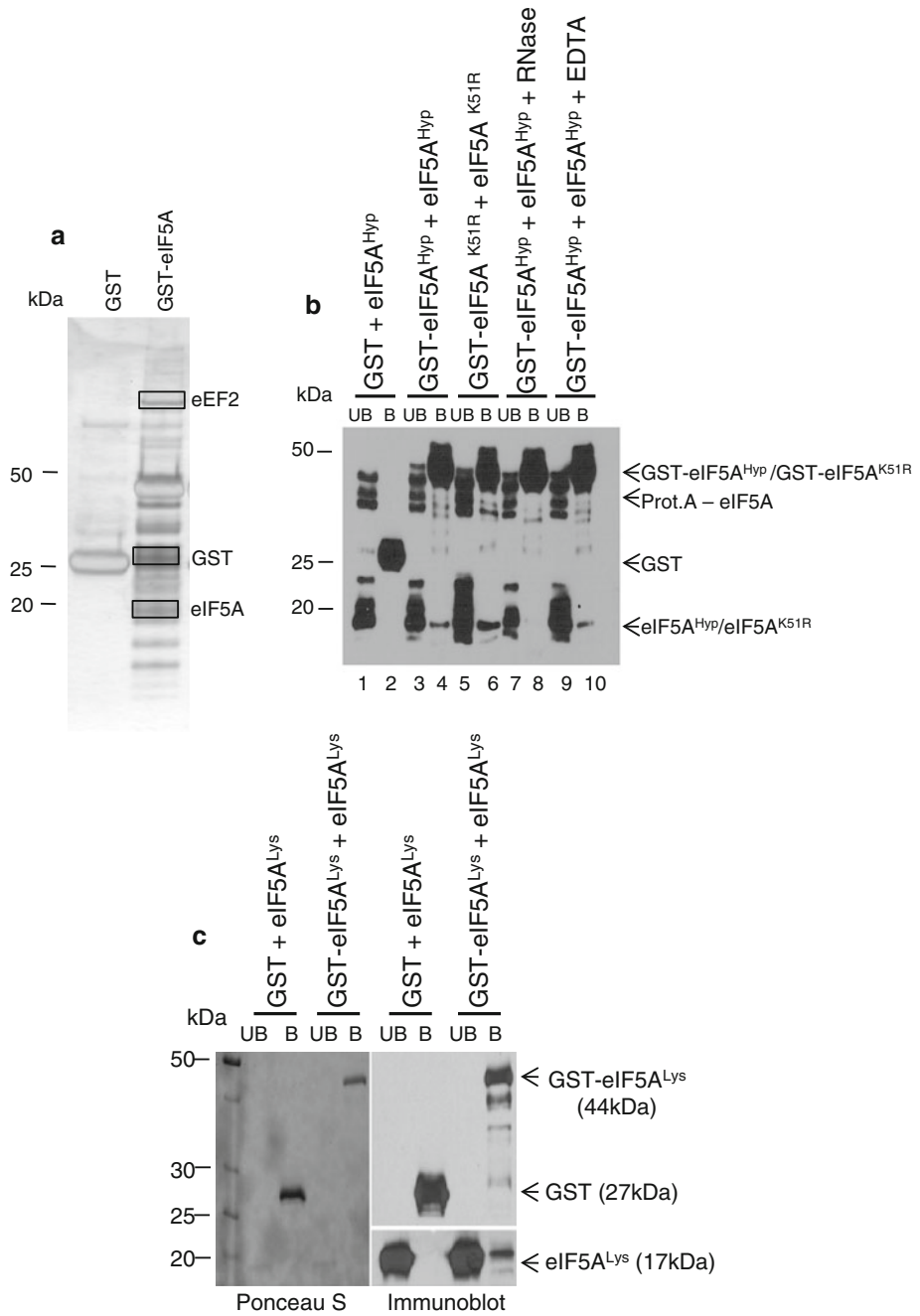

Fig. 3 Analysis of oligomeric state of eIF5A using GST pull-down assay. **a** Oligomeric state of eIF5A in vivo. Yeast whole cell extracts derived from cells expressing either GST (lane 1) or GST-eIF5A (lane 2) were incubated with glutathione Sepharose beads. After extensive washing, proteins bound to the beads were eluted, fractionated by SDS-PAGE and silver stained. Mass spectrometry analysis of excised protein bands revealed the copurified proteins as eEF2 and eIF5A (indicated by *squares*). In the same excised protein band of eIF5A, 40S ribosomal proteins S17-A (16KDa), S19-A (16KDa), S15 (16KDa), S18 (17KDa) and S26 (14KDa), and 60S ribosomal protein S20 (17KDa) were identified. GST was revealed only in the excised protein band corresponding to 26 kDa (indicated by *square*). **b** Yeast whole cell extracts derived from cells producing a tagged form of eIF5A (ProtA-eIF5A) and also expressing GST and eIF5A^{Hyp} (*lanes 1 and 2*), GST-eIF5A^{Hyp} and eIF5A^{Hyp} (lanes 3 and 4) and GST-eIF5A^{K51R} and eIF5A^{K51R} (*lanes 5 and 6*) were incubated with glutathione-Sepharose beads and subjected to pull-down assay. Proteins bound to the beads were eluted, fractionated by SDS-PAGE and analyzed by Western blot. UB and B refer to fractions unbound and bound to glutathione resin, respectively. The experiment using cells expressing GST-eIF5A^{Hyp} and eIF5A^{Hyp} was repeated in the presence of RNase (*lanes 7 and 8*) and EDTA (*lanes 9 and 10*). **c** Oligomeric state of eIF5A in vitro. The experiment described in (**b**) was conducted with GST, GST-eIF5A^{Lys} and eIF5A^{Lys} purified from *E. coli* (*right panel*), without ribosomal proteins, as revealed by Ponceau S (*left panel*)

oligonucleotide sequences (Xu and Chen 2001), and subsequent work identified some potential candidate target mRNAs (Xu et al. 2004). However, the biological significance of this supposed mRNA-binding capacity of eIF5A is as yet unknown. In addition, the presence of EDTA, which causes the dissociation of the 40S and 60S ribosomal subunits, did not affect the interaction between GST-eIF5A^{Hyp} and eIF5A^{Hyp} (Fig. 2a, lane 10), which indicates that the oligomeric state of eIF5A in vivo does not depend on the presence of assembled ribosomes or polysomes.

To confirm that the oligomeric state of eIF5A is independent of the hypusine modification and ribosomes, we performed an in vitro pull-down assay with purified proteins from *E. coli* (not containing the hypusine residue). As shown in Fig. 3c (Ponceau S—stained panel), it is clear that the proteins used (GST, GST-eIF5A^{Lys} and eIF5A^{Lys}) were pure, without any other bacterial proteins. The immunoblot panel (Fig. 3c) shows that GST-eIF5A^{Lys} interacts with eIF5A^{Lys} in this assay. Interestingly, the spectroscopic reading at 260 nm of the purified proteins showed that eIF5A^{Lys} was contaminated with RNA from bacteria (Online Resource Fig. 3c), indicating that the eIF5A oligomer in vitro is dependent on RNA and suggesting that the RNA necessary for dimerization is not specific. These findings are consistent with the result observed in Fig. 1d and also with previous published data showing the disruption of eIF5A dimer in vitro in the presence of RNase (Gentz et al. 2009).

eIF5A dimer is L-shaped and superimposable on tRNA^{Phe}, in a similar manner to the bacterial EF-P protein

Small-angle X-ray scattering (SAXS) is a technique suitable for the analysis of the overall shapes, dimensions and oligomeric states of macromolecules in solution (Svergun 1999; Batista et al. 2010). Therefore, SAXS measurements were used to probe the molecular shape of 6xHis-eIF5A^{Hyp} oligomers directly in solution. The X-ray scattering curve obtained for 6xHis-eIF5A^{Hyp} is shown in Fig. 4. The Guinier plot (Fig. 4a, inset) of the data exhibited a linear profile and the corresponding linear regression correlation coefficient was 0.997, indicating satisfactory monodispersity of 6xHis-eIF5A^{Hyp}. In agreement with other results presented, the radius of gyration calculated from the Guinier plot was Rg = 3.11 nm (Guinier 1955), which is very close to the value of 3.07 nm obtained from the integral analysis of the scattering curve using the method implemented in the Gnom package (Rg = 3.07 nm) (Svergun et al. 1988; Svergun 1999), both values being consistent with a dimeric molecule of eIF5A in solution. Ten independent ab initio simulations were performed with the Dammin package (Svergun 1999; Petoukhov and Svergun 2003) without imposing any symmetry restrictions, which reproduced well both the experimental curve and the pair distance distribution function $P(r)$. The reconstructed low-resolution model of 6xHis-eIF5A^{Hyp} restored at 2.10 nm resolution from synchrotron X-ray scattering data showed an elongated L-shaped molecule (Fig. 4b), with a maximum diameter of approximately 9.5 nm. This elongated molecular shape, shown in Fig. 4b, thus explains why size-exclusion chromatography tends to overestimate slightly the molecular mass of eIF5A dimer (40 kDa), which theoretically should be 34 kDa. The two SAXS-based methods used to calculate the molecular weight, which include absolute scattering intensity using water as primary standard (Orthaber et al. 2000), and the SAXS MoW web tool (Fischer et al. 2010), consistently reveal dimers of eIF5A in solution, with molecular weights of 38 and 35 kDa, respectively. The SAXS data are therefore consistent with a dimeric particle, supporting our proposal that eIF5A is a dimer in solution (Figs. 1, 2).

Figure 5 shows the SAXS experimental data and the computed scattering curves based on the crystallographic structures of eIF5A trimer from *Pyrococcus horikoshii* (PDB 1iz6), eIF5A dimer from *S. cerevisiae* (PDB ID 3er0), eIF5A dimer from human (PDB ID 3cpf) and eIF5A monomer from *Leishmania braziliensis* (PDB ID 1x6o). The scattering curve computed based on the crystallographic structure of eIF5A dimer from *S. cerevisiae* exhibited the best fit to the experimental data, compared to the other scattering curves (Fig. 5, black solid line). However, the eIF5A dimer model needs to be more elongated than the crystallographic structure (PDB ID 3er0) to fit the experimental SAXS data. The radius of gyration calculated from the crystallographic structure was 2.50 nm (Online Resource Table 3), which is smaller than the value obtained from experimental data (Rg = 3.11 nm). Thus, we performed rigid-body adjustments of the crystallographic model, based on our SAXS curve (Figs. 4a, 6). The two monomers from the crystallographic structure were separated and the resulting rigid-body model showed a more elongated dimer. Figure 6 shows the superposition of the crystallographic structure of eIF5A (PDB ID 3er0) on the rigid-body model. The rigid-body adjustments of the eIF5A dimer resulted in a considerably better fit to SAXS experimental data (Fig. 4a, gray line). Superposition of the low-resolution model and eIF5A dimer rigid-body model shows good agreement (Fig. 4b) and it is clear that the SAXS model of eIF5A is compatible with two eIF5A molecules. However, by the assays described here, it is not possible to know if the relative disposition of the two molecules of eIF5A in the rigid-body model is indeed the same of the 6xHis-eIF5A^{Hyp} dimer in solution. A summary of the main results described in this study is given in Online Resource Table 3.

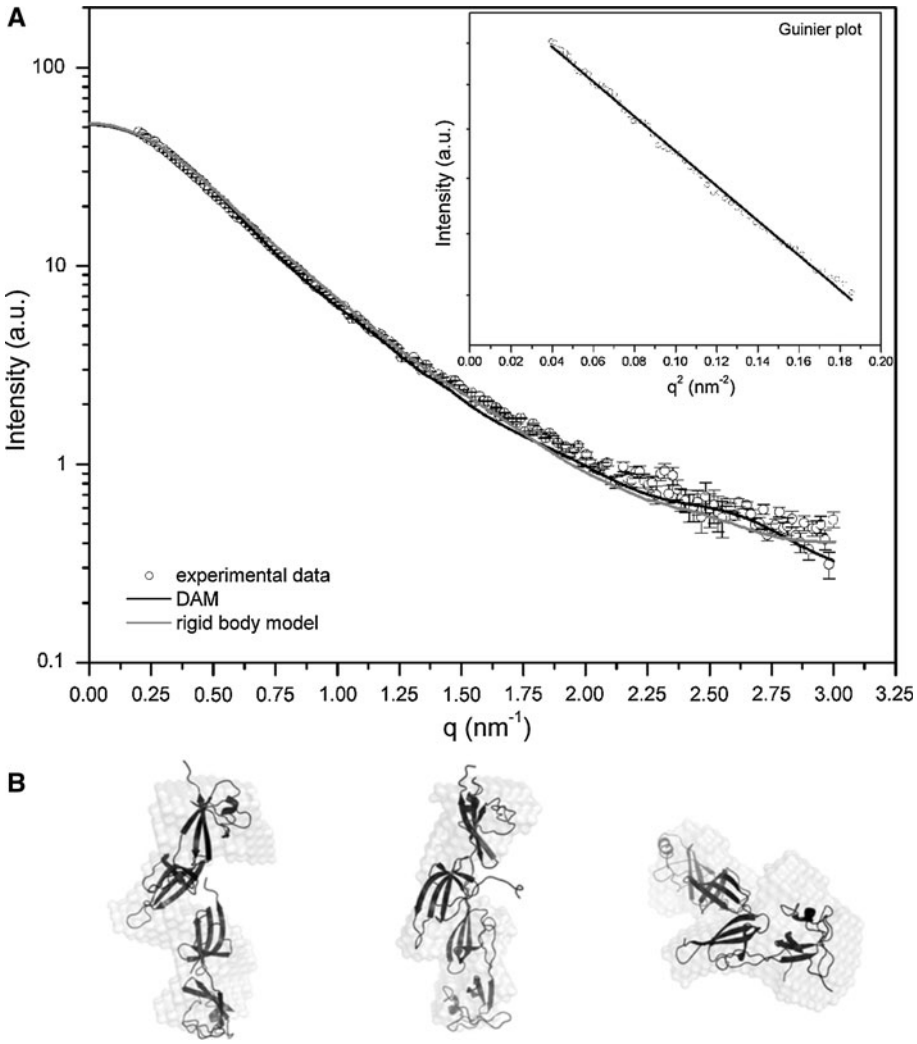

Fig. 4 Overall shape, dimensions and oligomeric state of eIF5A in solution by small-angle X-ray scattering (SAXS). **a** Experimental solution scattering curve of 6xHis-eIF5A^{Hyp} (ln I versus q) (*open black circles with error bars*) superimposed on the computed scattering curves based on the restored low-resolution model (*black solid line*) and the rigid-body model (*gray line*). *Inset* Guinier plot (ln I versus q^2). The radius of gyration obtained from the Guinier plot is 3.11 nm, just slightly bigger than 3.07 nm obtained from the integral analyses of the scattering curve by the method implemented in Gnom. **b** Molecular envelope of 6xHis-eIF5A^{Hyp} in solution was restored from synchrotron X-ray scattering data with an ab initio simulated annealing algorithm implemented in the Dammin package. Only the best model is shown. Two molecules of 6xHis-eIF5A^{Hyp} from *S. cerevisiae* (rigid-body model) were aligned with the low-resolution model generated by SAXS, using Supcomp 20 software

eIF5A shares sequence and structural similarity with the first two domains of EF-P. Domain I of EF-P is topologically the same as the N-terminal domain of eIF5A. On the other hand, EF-P domains II and III each share the same topology as that of the eIF5A C-terminal domain, indicating that domains II and III arose by duplication (Hanawa-Suetsugu et al. 2004). However, in contrast to eIF5A, which is a dimer in solution (Figs. 1, 2, 4), EF-P exists as a monomer under physiological conditions (Hanawa-Suetsugu et al. 2004). To verify whether the EF-P monomer and eIF5A dimer have similar overall shapes, we conducted structural alignment between the crystallographic structures of EF-P monomer and the SAXS low-resolution model of eIF5A (Fig. 7). Figure 7a shows the SAXS experimental data and the scattering curves computed based on the crystallographic structures of EF-P monomer (PDB ID 1ueb) and tRNA^{Phe} (PDB ID 4tna). Although eIF5A is composed of approximately 140 amino acid residues and is shorter than EF-P by approximately 40 residues, we can see, in Fig. 7b, that the low-resolution model of eIF5A dimer (maximum dimension of approximately 9.5 nm and Rg = 3.12 nm) is bigger than the EF-P monomer (maximum dimension of approximately 8 nm and Rg = 2.20 nm) (Online Resource Table 3). Interestingly, the shapes of the eIF5A dimer and EF-P monomer are superimposable and the angle formed between EF-P domains I and II is similar to the angle existing in the eIF5A low-resolution model (Fig. 7b).

The crystal structure of EF-P monomer showed that its overall shape and dimensions are strikingly similar to those of tRNAs (Hanawa-Suetsugu et al. 2004; Choi and Choe 2011). Figure 7c, d shows the crystal structure of tRNA^{Phe} from *S. cerevisiae* (PDB ID 4tna) and its structural alignment with the monomer of the EF-P crystal structure (PDB ID 1ueb), respectively. Interestingly, we can see in Fig. 7e that the SAXS low-resolution model of the eIF5A dimer is superimposable on the tRNA^{Phe} structure (maximum dimension of approximately 8. 85 nm and Rg = 2.34 nm) (Online Resource Table 3),

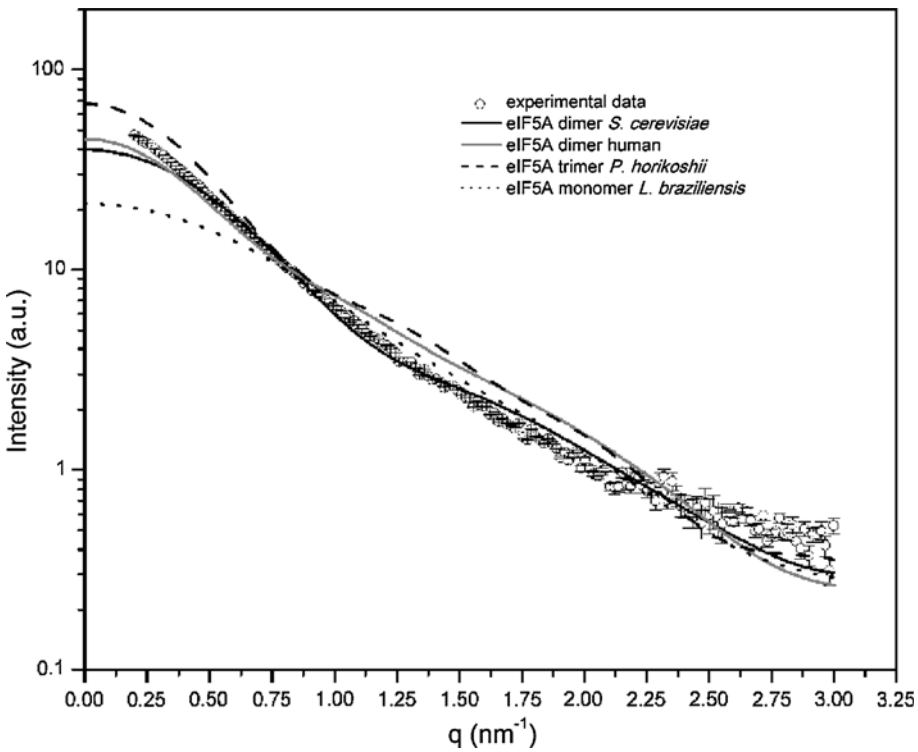

Fig. 5 Small-angle X-ray scattering (SAXS) curves. Experimental solution scattering curve of 6xHis-eIF5A^{Hyp} (ln I versus *q*) (*open black circles with error bars*) superimposed on the computed scattering curves based on the crystallographic structures (high-resolution model) of eIF5A trimer from *Pyrococcus horikoshii* (PDB 1iz6) (*dashed line*), eIF5A dimer from *Saccharomyces cerevisiae* (PDB ID 3er0) (*black solid line*), eIF5A dimer from human (PDB ID 3cpf) (*gray line*) and eIF5A monomer from *Leishmania braziliensis* (PDB ID 1x6o) (*dotted line*)

Fig. 6 Rigid-body model. Superposition of the rigid-body model (*gray*) on the crystallographic structure (PDB ID 3er0) (*black*), showing the modification imposed on the rigid-body model being more elongated than the crystallographic structure

as is the EF-P monomer. In fact, many of the translation factors (initiation, elongation, release and recycling factors) mimic the shape of tRNA (Nakamura and Ito 2003; Vestergaard et al. 2001; Lancaster et al. 2002). This structural similarity, however, does not necessarily indicate that these factors bind to the ribosome in the same way as tRNAs. EF-P, for example, binds between the E- and P-sites, which differs from classical tRNA binding sites (Blaha et al. 2009).

A variety of functions has been proposed for eIF5A, but its mode of action remains unclear (Henderson and Hershey 2011). Although the interaction between the ribosome and eIF5A has been described by several groups (Jao and Chen 2006; Zanelli et al. 2006; Gregio et al. 2009; Saini et al. 2009), we do not know yet where eIF5A binds on the ribosome. Here, we have shown strong evidence that eIF5A may be a dimer in vivo, independently of the hypusine residue or whole ribosome, but dependent on RNA. Furthermore, we showed that eIF5A dimer is L-shaped and superimposable on tRNA^{Phe}, similarly to the EF-P monomer. Additional studies are necessary to know if the eIF5A dimer is functional and essential for cell growth. However, since eIF5A shows high structural similarity to EF-P and both enhance the rate of formation of the first peptide bond, we propose that two molecules of eIF5A may be necessary in eukaryotes to perform the same role that one molecule of EF-P does in bacteria.

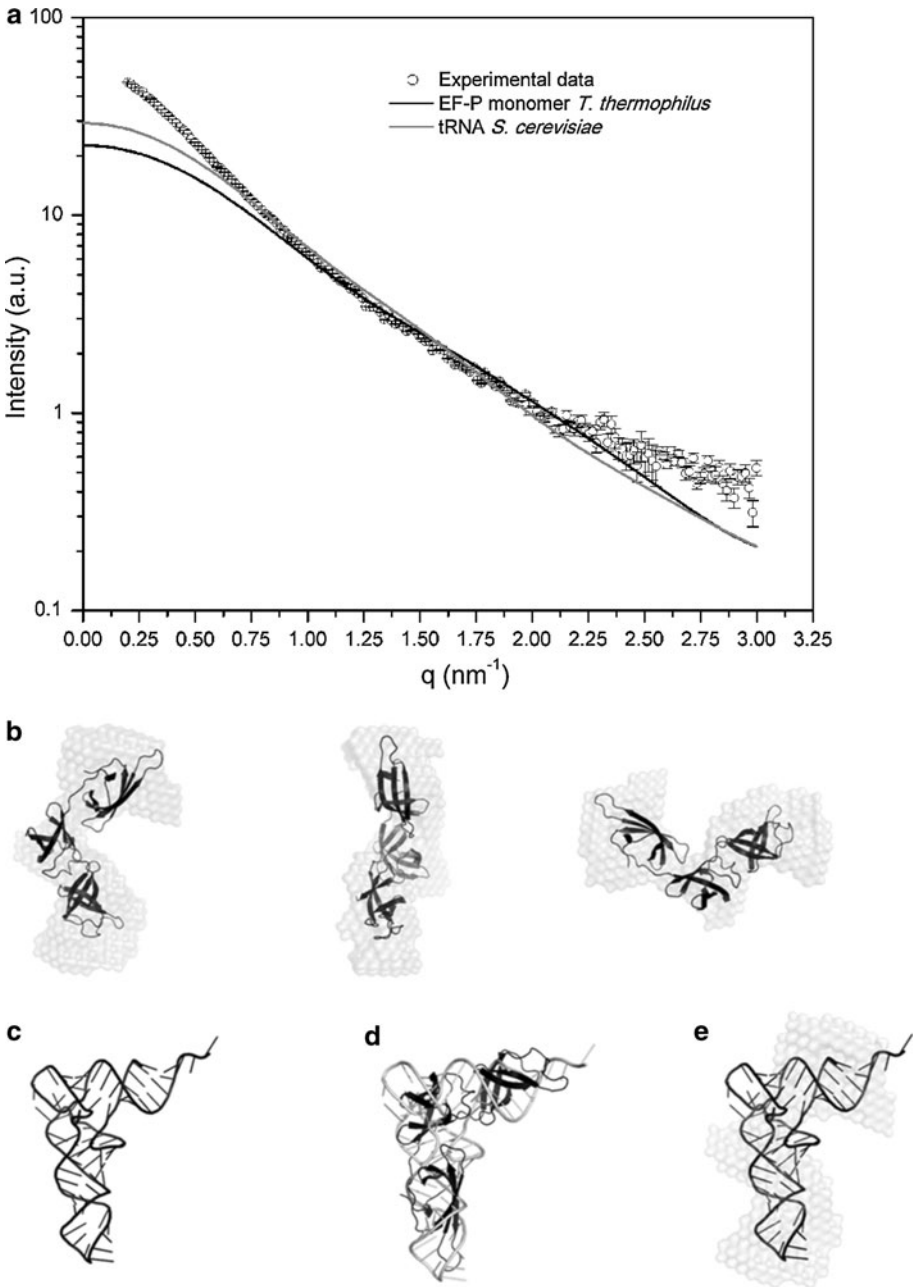

Fig. 7 Comparative analyses of molecular envelopes of 6xHis-eIF5A^{Hyp}, EF-P monomer and tRNA^{Phe}. **a** Experimental solution scattering curve of 6xHis-eIF5A^{Hyp} (ln I versus *q*) (*open black circles with error bars*) superimposed on the computed scattering curves based on the crystallographic structures (high-resolution model) of EF-P monomer (PDB ID 1ueb) (*black solid line*) and tRNA^{Phe} (PDB ID 4tna) (*gray line*). **b** Structural alignment of the molecular envelope of 6xHis-eIF5A^{Hyp} dimer and EF-P monomer. **c** tRNA^{Phe} from *S. cerevisiae*. **d** Structural alignment of tRNA^{Phe} from *S. cerevisiae* and EF-P monomer from *T. thermophilus*. **e** Structural alignment of the molecular envelope of 6xHis-eIF5A^{Hyp} dimer and tRNA^{Phe} from *S. cerevisiae*

Acknowledgments This work was supported by grants to S.R.V. from Fundação de Amparo à Pesquisa do Estado de São Paulo (FAPESP), Conselho Nacional de Desenvolvimento Científico e Tecnológico (CNPq) and Faculdade de Ciências Farmacêuticas (PADC). We also thank FAPESP and CNPq for the fellowship awarded to Camila A. O. Dias. We would like to thank the staff of the National Synchrotron Light Laboratory (LNLS, Brazil) for access to the SAXS beamline and other facilities.

References

Bailly M, de Crécy-Lagard V (2010) Predicting the pathway involved in post-translational modification of elongation factor P in a subset of bacterial species. Biol Direct 5:3

Batista FA, Goto LS, Garcia W, de Moraes DI, de Oliveira Neto M, Polikarpov I, Cominetti MR, Selistre-de-Araújo HS, Beltramini LM, Araújo AP (2010) Camptosemin, a tetrameric lectin of *Camptosema ellipticum*: structural and functional analysis. Eur Biophys J 39(8):1193–1205

Benne R, Hershey JW (1978) The mechanism of action of protein synthesis initiation factors from rabbit reticulocytes. J Biol Chem 253(9):3078–3087

Blaha G, Stanley RE, Steitz TA (2009) Formation of the first peptide bond: the structure of EF-P bound to the 70S ribosome. Science 325(5943):966–970

Chen KY, Liu AY (1997) Biochemistry and function of hypusine formation on eukaryotic initiation factor 5A. Biol Signals 6(3):105–109

Choi S, Choe J (2011) Crystal structure of elongation factor P from *Pseudomonas aeruginosa* at 1.75 A resolution. Proteins 79(5):1688–1693

Chung SI, Park MH, Folk JE, Lewis MS (1991) Eukaryotic initiation factor 5A: the molecular form of the hypusine-containing protein from human erythrocytes. Biochim Biophys Acta 1076(3):448–451

Delano WL (2002) The PyMOL molecular graphics system delano scientific

Dias CA, Cano VS, Rangel SM, Apponi LH, Frigieri MC, Muniz JR, Garcia W, Park MH, Garratt RC, Zanelli CF, Valentini SR (2008) Structural modeling and mutational analysis of yeast eukaryotic translation initiation factor 5A reveal new critical residues and reinforce its involvement in protein synthesis. FEBS J 275(8):1874–1888

Dias CA, Gregio APB, Rossi D, Galvão FC, Watanabe TF, Park MH, Valentini SR, Zanelli CF (2012) eIF5A interacts functionally with eEF2. Amino Acids 42(2–3):697–702

Fischer H, de Oliveira Neto M, Napolitano HB, Polikarpov I, Craievich AF (2010) Determination of the molecular weight of proteins in solution from single small-angle X-ray scattering measurement on a relative scale. J Appl Cryst 43:101–109

Frigieri MC, Thompson GM, Pandolfi JR, Zanelli CF, Valentini SR (2007) Use of a synthetic lethal screen to identify genes related to TIF51A in *Saccharomyces cerevisiae*. Genet Mol Res 6(1):152–165

Frigieri MC, Joao Luiz MV, Apponi LH, Zanelli CF, Valentini SR (2008) Synthetic lethality between eIF5A and Ypt1 reveals a connection between translation and the secretory pathway in yeast. Mol Genet Genomics 280(3):211–221

Gentz PM, Blatch GL, Dorrington RA (2009) Dimerization of the yeast eukaryotic translation initiation factor 5A requires hypusine and is RNA dependent. FEBS J 276(3):695–706

Glick BR, Chladek S, Ganoza MC (1979) Peptide bond formation stimulated by protein synthesis factor EF-P depends on the aminoacyl moiety of the acceptor. Eur J Biochem/FEBS 97(1):23–28

Gough J, Karplus K, Hughey R, Chothia C (2001) Assignment of homology to genome sequences using a library of hidden Markov models that represent all proteins of known structure. J Mol Biol 313(4):903–919

Gregio AP, Cano VP, Avaca JS, Valentini SR, Zanelli CF (2009) eIF5A has a function in the elongation step of translation in yeast. Biochem Biophys Res Commun 380(4):785–790

Guinier A (1955) Small-angle scattering of X-rays. In: Fournet G, ed. John Wiley and Sons, New York

Hammerley AP (1997) FIT2D: An introduction and Overview. ESRF International Report

Hanawa-Suetsugu K, Sekine S, Sakai H, Hori-Takemoto C, Terada T, Unzai S, Tame JR, Kuramitsu S, Shirouzu M, Yokoyama S (2004) Crystal structure of elongation factor P from *Thermus thermophilus* HB8. Proc Nat Acad Sci USA 101(26):9595–9600

Henderson A, Hershey JW (2011) The role of eIF5A in protein synthesis. Cell Cycle 10(21):3617–3618

Hershey JW, Smit-McBride Z, Schnier J (1990) The role of mammalian initiation factor eIF-4D and its hypusine modification in translation. Biochim Biophys Acta 1050(1–3):160–162

Jao DL, Chen KY (2006) Tandem affinity purification revealed the hypusine-dependent binding of eukaryotic initiation factor 5A to the translating 80S ribosomal complex. J Cell Biochem 97(3):583–598

Kang HA, Hershey JW (1994) Effect of initiation factor eIF-5A depletion on protein synthesis and proliferation of *Saccharomyces cerevisiae*. J Biol Chem 269(6):3934–3940

Kellermann G, Vicentin F, Tamura E, Rocha M, Tolentino H, Barbosa A, Craievich A, Torriani I (1997) The small-angle X-ray scattering beamline of the Brazilian Synchrotron Light Laboratory. J Appl Crystallogr 30(2):880–883

Kemper WM, Berry KW, Merrick WC (1976) Purification and properties of rabbit reticulocyte protein synthesis initiation factors M2Balpha and M2Bbeta. J Biol Chem 251(18): 5551–5557

Konarev PV (2006) ATSAS 2.1, a program package for small-angle scattering data analysis. J Appl Cryst 39:277–286

Kozin MB, Svergun DI (2001) Automated matching of high- and low-resolution structural models. J Appl Crystallogr 34:33–41

Lancaster L, Kiel MC, Kaji A, Noller HF (2002) Orientation of ribosome recycling factor in the ribosome from directed hydroxyl radical probing. Cell 111(1):129–140

Nakamura Y, Ito K (2003) Making sense of mimic in translation termination. Trends Biochem Sci 28(2):99–105

Navarre WW, Zou SB, Roy H, Xie JL, Savchenko A, Singer A, Edvokimova E, Prost LR, Kumar R, Ibba M, Fang FC (2010) PoxA, yjeK, and elongation factor P coordinately modulate virulence and drug resistance in *Salmonella enterica*. Mol Cell 39(2):209–221

Orthaber D, Bergmann A, Glatter O (2000) SAXS experiments on absolute scale with Kratky systems using water as a secondary standard. J Appl Cryst 33:218–225

Park MH, Wolff EC, Folk JE (1993) Is hypusine essential for eukaryotic cell proliferation? Trends Biochem Sci 18(12):475–479

Park MH, Lee YB, Joe YA (1997) Hypusine is essential for eukaryotic cell proliferation. Biol Signals 6(3):115–123

Park MH, Nishimura K, Zanelli CF, Valentini SR (2010) Functional significance of eIF5A and its hypusine modification in eukaryotes. Amino Acids 38(2):491–500

Park JH, Dias CA, Lee SB, Valentini SR, Sokabe M, Fraser CS, Park MH (2011) Production of active recombinant eIF5A: reconstitution in *E. coli* of eukaryotic hypusine modification of eIF5A by its coexpression with modifying enzymes. Protein Eng Des Sel 24(3):301–309

Park JH, Johansson HE, Aoki H, Huang BX, Kim HY, Ganoza MC, Park MH (2012) Post-translational modification by β-lysylation is required for activity of *Escherichia coli* elongation factor P (EF-P). J Biol Chem 287(4):2579–2590

Petoukhov MV, Svergun DI (2003) New methods for domain structure determination of proteins from solution scattering data. J Appl Crystallogr 36:540–544

Prinz B, Schultchen J, Rydzewski R, Holz C, Boettner M, Stahl U, Lang C (2004) Establishing a versatile fermentation and purification procedure for human proteins expressed in the yeasts *Saccharomyces cerevisiae* and *Pichia pastoris* for structural genomics. J Struct Funct Genomics 5(1–2):29–44

Roy H, Zou SB, Bullwinkle TJ, Wolfe BS, Gilreath MS, Forsyth CJ, Navarre WW, Ibba M (2011) The tRNA synthetase paralog PoxA modifies elongation factor-P with (R)-beta-lysine. Nat Chem Biol 7(10):667–669

Saini P, Eyler DE, Green R, Dever TE (2009) Hypusine-containing protein eIF5A promotes translation elongation. Nature 459 (7243):118–121

Schnier J, Schwelberger HG, Smit-McBride Z, Kang HA, Hershey JW (1991) Translation initiation factor 5A and its hypusine modification are essential for cell viability in the yeast *Saccharomyces cerevisiae*. Mol Cell Biol 11(6):3105–3114

Svergun D (1992) Determination of the regularization parameter in indirect-transform methods using perceptual criteria. J Appl Cryst 25:495–503

Svergun DI (1999) Restoring low resolution structure of biological macromolecules from solution scattering using simulated annealing. Biophys J 76(6):2879–2886

Svergun D, Petoukhov Koch M (2001) Determination of domain structure of proteins from X-ray solution scattering. Biophys J 80:2946–2953

Svergun DI, Semenyuk AV, Feigin LA (1988) Small-angle-scattering-data treatment by the regularization method. Acta Crystallogr A 44:244–250

Tong Y, Park I, Hong BS, Nedyalkova L, Tempel W, Park HW (2009) Crystal structure of human eIF5A1: insight into functional similarity of human eIF5A1 and eIF5A2. Proteins 75(4):1040–1045

Vestergaard B, Van LB, Andersen GR, Nyborg J, Buckingham RH, Kjeldgaard M (2001) Bacterial polypeptide release factor RF2 is structurally distinct from eukaryotic eRF1. Mol Cell 8(6): 1375–1382

William KR, Lopresti M, Stone K (1997) Internal protein sequencing of SDS-PAGE separated proteins: optimization of an in-gel digest protocol. In: Marshak D (ed) Techniques VIII. Academic Press, San Diego, pp 79–90

Xu A, Chen KY (2001) Hypusine is required for a sequence-specific interaction of eukaryotic initiation factor 5A with post systematic evolution of ligands by exponential enrichment RNA. J Biol Chem 276(4):2555–2561

Xu A, Jao DL, Chen KY (2004) Identification of mRNA that binds to eukaryotic initiation factor 5A by affinity co-purification and differential display. Biochem J 384(Pt 3):585–590

Yanagisawa T, Sumida T, Ishii R, Takemoto C, Yokoyama S (2010) A paralog of lysyl-tRNA synthetase aminoacylates a conserved lysine residue in translation elongation factor P. Nat Struct Mol Biol 17(9):1136–1143

Zanelli CF, Valentini SR (2005) Pkc1 acts through Zds1 and Gic1 to suppress growth and cell polarity defects of a yeast eIF5A mutant. Genetics 171(4):1571–1581

Zanelli CF, Maragno AL, Gregio AP, Komili S, Pandolfi JR, Mestriner CA, Lustri WR, Valentini SR (2006) eIF5A binds to translational machinery components and affects translation in yeast. Biochem Biophys Res Commun 348(4):1358–1366